LEARNING TO OBSERVE WITH REINFORCEMENT LEARNING

Anonymous authors
Paper under double-blind review

ABSTRACT

We consider a decision making problem where an autonomous agent decides on which actions to take based on the observations it collects from the environment. We are interested in revealing the information structure of the observation space illustrating which type of observations are the most important (such as position versus velocity) and the dependence of this on the state of agent (such as at the bottom versus top of a hill). We approach this problem by associating a cost with collecting observations which increases with the accuracy. We adopt a reinforcement learning (RL) framework where the RL agent learns to adjust the accuracy of the observations alongside learning to perform the original task. We consider both the scenario where the accuracy can be adjusted continuously and also the scenario where the agent has to choose between given preset levels, such as taking a sample perfectly or not taking a sample at all. In contrast to the existing work that mostly focuses on sample efficiency during training, our focus is on the behaviour during the actual task. Our results illustrate that the RL agent can learn to use the observation space efficiently and obtain satisfactory performance in the original task while collecting effectively smaller amount of data. By uncovering the relative usefulness of different types of observations and trade-offs within, these results also provide insights for further design of active data acquisition schemes.

1 INTRODUCTION

Autonomous decision making relies on collecting data, i.e. observations, from the environment where the actions are decided based on the observations. We are interested in revealing the information structure of the observation space illustrating which type of observations are the most important (such as position versus velocity). Revealing this structure is challenging since the usefulness of the information that an observation can bring is a priori unknown and depends on the environment as well as the current knowledge state of the decision-maker, for instance, whether the agent is at the bottom versus the top of a hill and how sure the agent is about its position. Hence, we're interested in questions such as "Instead of collecting all available observations, is it possible to skip some observations and obtain satisfactory performance?", "Which observation components (such as the position or the velocity) are most useful when the object is far away from (or close to) the target state?". The aim of this work is to reveal this information structure of the observation space within a systematic framework.

We approach this problem by associating a cost with collecting observations which increases with the accuracy. The agent can choose the accuracy level of its observations. Since cost increases with the accuracy, we expect that the agent will choose to collect only the observations which are most likely to be informative and worth the cost. We adopt a reinforcement learning (RL) framework where the RL agent learns to adjust the accuracy of the observations alongside learning to perform the original task. We consider both the scenario where the accuracy can be adjusted continuously and also the scenario where the agent has to choose between given preset levels, such as taking a sample perfectly or not taking a sample at all. In contrast to the existing work that mostly focuses on sample efficiency during training, our focus is on the behaviour during the actual task. Our results illustrate that the RL agent can learn to use the observation space efficiently and obtain satisfactory performance in the original task while collecting effectively smaller amount of data.

2 RELATED WORK

A related setting is active learning (Settles, 2010; Donmez et al., 2010) where an agent decides which queries to perform, i.e., which samples to take, during training. For instance, in active learning set-up, an agent learning to classify images can decide which images from a large dataset it would like to have labels for in order to have improved classification performance. In a standard active learning approach (Settles, 2010; Donmez et al., 2010) as well as its extensions in RL (Lopes et al., 2009), the main aim is to reduce the size of the training set, hence the agent tries to determine informative queries during training so that the performance during the test phase is optimal. In the test phase, the agent cannot ask any questions; instead, it will answer questions, for instance, it will be given images to label. In contrast, in our setting the agent continues to perform queries during the test phase, since it still needs to collect observations during the test phase, for instance as in the case of collecting camera images for an autonomous driving application. From this perspective, one of our main aims is to reduce the number of queries the agent performs during this actual operation.

Another related line of work consists of the RL approaches that facilitate efficient exploration of state space, such as curiosity-driven RL and intrinsic motivation (Pathak et al., 2017; Bellemare et al., 2016; Mohamed & Rezende, 2015; Still & Precup, 2012) or active-inference based methods utilizing free-energy (Ueltzhöffer, 2018; Schwöbel et al., 2018); and the works that focus on operation with limited data using a model (Chua et al., 2018; Deisenroth & Rasmussen, 2011; Henaff et al., 2018; Gal et al., 2016). In these works, the focus is either finding informative samples (Pathak et al., 2017) or using a limited number of samples/trials as much as possible by making use of a forward dynamics model (Boedecker et al., 2014; Chua et al., 2018; Deisenroth & Rasmussen, 2011; Henaff et al., 2018; Gal et al., 2016) during the agent's training. In contrast to these approaches, we would like to decrease the effective size of the data or the number of samples taken during the test phase, i.e. actual operation of the agent.

Representation learning for control and RL constitutes another line of related work (Watter et al., 2015; Hafner et al., 2019; Banijamali et al., 2018). In these works, the transformation of the observation space to a low-dimensional space is investigated so that action selection can be performed using this low-dimensional space. Similar to these works, our framework can be also interpreted as a transformation of the original observation space where an effectively low-dimensional space is sought after. Instead of allowing a general class of transformations on the observations, here we consider a constrained setting so that only specific operations are allowed, for instance, we allow dropping some of the samples but we do not allow collecting observations and then applying arbitrary transformations on them.

3 PROPOSED FRAMEWORK AND THE SOLUTION APPROACH

3.1 PRELIMINARIES

Consider a Markov decision process (MDP) given by $\langle \mathcal{S}, \mathcal{A}, \mathcal{P}, R, P_{s_0}, \gamma \rangle$ where $\mathcal{S}$ is the state space, $\mathcal{A}$ is the set of actions, $\mathcal{P} : \mathcal{S} \times \mathcal{A} \times \mathcal{S} \to \mathbb{R}$ denotes the transition probabilities, $R : \mathcal{S} \times \mathcal{A} \to \mathbb{R}$ denotes the bounded reward function, $P_{s_0} : \mathcal{S} \to \mathbb{R}$ denotes the probability distribution over the initial state and $\gamma \in (0, 1]$ is the discount factor.

The agent, i.e. the decision maker, observes the state of the system s_t at time t and decides on its action a_t based on its policy $\pi(s, a)$. The policy mapping of the agent $\pi(s, a) : \mathcal{S} \times \mathcal{A} \to [0, 1]$ is possibly stochastic and gives the probability of taking the action a at a state s. After the agent implements the action a_t, it receives a reward $r(s_t, a_t)$ and the environment moves to the next state s_{t+1} which is governed by $\mathcal{P}$ and depends on a_t and s_t. The aim of the RL agent is to learn an optimal policy mapping $\pi(s, a)$ so that the expected return, i.e. expected cumulative discounted reward, $J(\pi) = \mathbb{E}_{a_t \sim \pi, s_t \sim P}[\sum_t \gamma^t r(s_t, a_t)]$ is maximized.

3.2 PARTIAL OBSERVABILITY

Although most RL algorithms are typically expressed in terms of MDPs, in typical real-life applications the states are not directly observable, i.e., the observations only provide partial, possibly inaccurate information. For instance, consider a vehicle which uses the noisy images with limited

angle-of-view obtained from cameras mounted on the vehicle for autonomous-driving decisions. In such scenarios, the data used by the agent to make decisions is not a direct representation of the state of the world. Hence, we consider a partially observable Markov decision process (POMDP) where the above MDP is augmented by $\mathcal{O}$ and $\mathcal{P}_o$ where $\mathcal{O}$ represents the set of observations and $\mathcal{P}_o : \mathcal{S} \rightarrow \mathcal{O}$ represents the observation probabilities. Accordingly, the policy mapping is now expressed as $\pi(o, a) : \mathcal{O} \times \mathcal{A} \rightarrow [0, 1]$.

Observation vector at time t is given by $o_t = [o_t^1; \ldots; o_t^n] \in \mathbb{R}^n$, where n is the dimension of the observation vector. The observations are governed by

$$o_t \sim p_o(o_t|s_t; \beta_t) \tag{1}$$

where $p_o(o_t|s_t; \beta_t)$ denotes the conditional probability distribution function (pdf) of o_t given s_t and is parametrized by the accuracy vector

$$\beta_t = [\beta_t^1; \ldots; \beta_t^n] \in \mathbb{R}^n \tag{2}$$

The parameter $\beta_t^i \geq 0$ represents the average accuracy of the observation component i at time step t, i.e. o_t^i. For instance, say we have two observations, position o^1 and velocity o^2. Then, β_t^1 denotes the accuracy of the position and β_t^2 denotes the accuracy of the velocity. As β_t^i increases, the accuracy of the observation o_t^i decreases. Given s_t and β_t, the observations are statistically independent, i.e. we have the factorization

$$p_o(o_t|s_t; \beta_t) = \prod_{i=1,\ldots,n} p_{o^i}(o_t^i|s_t; \beta_t^i) \tag{3}$$

where $p_{o^i}(o_t^i|s_t; \beta_t^i)$ denotes the conditional pdf of o_t^i given s_t and β_t^i.

Note that β_t^i determines the average accuracy, i.e. the accuracy in the statistical sense. We provide an example below:

Example: Consider the common Gaussian additive noise model with

$$o_t^i = s_t^i + v_t^i, \qquad i = 1, \ldots, n, \tag{4}$$

where $s_t = [s_t^1; \ldots; s_t^n] \in \mathbb{R}^n$ is the state vector and $v_t = [v_t^1; \ldots; v_t^n] \in \mathbb{R}^n$ is the Gaussian noise vector with $\mathcal{N}(0, \text{diag}(\sigma^2_{v_t^i}))$. Here, v_t and v_t' are statistically independent (stat. ind.) for all $t \neq t'$ and also v_t and s_t' are stat. ind. for all t, t'. Under this observation model, a reasonable choice for β_t^i is $\beta_t^i = \sigma^2_{v_t^i}$. Hence, we parametrize $p_o^i(.)$ as $p_o^i(o_t^i|s_t^i; \beta_t^i) = \mathcal{N}(s_t^i, \beta_t^i = \sigma^2_{v_t^i})$. Note that the parametrization in terms of β_t^i can be done in multiple ways, for instance, one may also adopt $\beta_t^i = \sigma_{v_t^i}$.

3.3 Decision maker chooses the accuracy of the observations

The agent can choose β_t^i, hence β_t^i is a decision variable. Observations have a cost which increases with increasing accuracy, i.e. the cost increases with decreasing β_t^i.

- In Scenario A, the agent can vary β_t^i on a continuous scale, i.e. $\beta_t^i \in [0, \infty]$.
- In Scenario B, the agent chooses between i) collecting all the observations with a fixed level of accuracy or ii) not getting it at all. This setting corresponds to the case with $\bar{\beta}_t \in \{\beta_0, \infty\}$ where $\beta_0 \geq 0$ represents a fixed accuracy level. Note that β_0 can be zero, corresponding to the case $o_t = s_t$.

3.3.1 Motivation

This framework is designed to reveal the inherent nature of observation space in terms of usefulness of information the observations provide with respect to the task at hand. In particular, when the cost of the observations increase with the accuracy, only the observation components (or the observation vectors) which are mostly likely to be informative and worth the cost will be collected. This decision heavily depends on the state that the agent believes itself to be in. For instance, in the case of balancing an object at an unstable state (such as pendulum in OpenAi Gym (Brockman et al., 2016)), we intuitively expect that the agent does not need accurate measurements when it is far away from

the target state. Hence, we're interested in questions such as "Is it possible to skip some observations and obtain satisfactory performance?", "Which observation components (such as the position or the velocity) are most useful when the object is far away from (or close to) the target state?", "How are these results affected by the possible discrepancy between the true state the agent is in and the one that it believes it to be in due to noisy or skipped observations?". The aim of the proposed framework is to reveal this information structure within a systematic setting.

Remark 3.1 This setting can be interpreted as a constrained representation learning problem for RL. In particular, consider the problem of learning the best mapping $h(.)$ with

$$z_t = h(\bar{o}_t) \tag{5}$$

from the high-dimensional original observations $\bar{o}_t$ to some new possibly low-dimensional variables z_t so that control can be performed reliably on z_t instead of $\bar{o}_t$. Such settings have been utilized in various influential work, see for instance E2C approach of Watter et al. (2015).

The proposed approach can be also formulated in a representation framework. In particular, we interpret the possibly noisy observations o_t as the effectively low-dimensional representation z_t used in (5). Hence, consider the mapping $\bar{h}(.)$

$$o_t = \bar{h}(\bar{o}_t) \tag{6}$$

where o_t denotes the noisy measurements and $\bar{o}_t$ denotes the original measurements. Compared to (5), the family of the mappings allowed in (6) is constrained, i.e. one can only adjust the accuracy parameter instead of allowing arbitrary transformations from $\bar{o}_t$ to o_t. Here, o_t is effectively low-dimensional compared to $\bar{o}_t$ because i) the noise decreases the dynamic range, and for instance allows effectively higher compression rates of the data (Scenario A); or ii) the total number of observations acquired is smaller (Scenario B).

Note that not all transformations from the state s_t to the observations o_t can be written using (6) as an intermediate step. From this perspective, the formulation in (1) can be said to be more general than (6).

Examples: In addition to revealing the information structure of the observation space, the proposed scenarios A and B also correspond to practical data acquisition schemes. We now give some examples:

An example for Scenario A, the case where is the observations are obtained using different sensors on the device where the accuracy of each sensor can be individually adjusted. Another example is the case where the sensors are distributed over the environment and the readings of the sensors has to be relayed to central decision unit using individual compression of each observation type and wireless communications. Here, the compression and the wireless communication introduces an accuracy-cost trade-off where the agent can choose to operate at different points of. Please see Section A.1 for an example illustrating the accuracy-cost trade-off in wireless communications.

An example for Scenario B is the remote control of a device, such as a drone, where all sensor readings of the device are compressed together and then sent to a decision unit. Since all readings are compressed and transmitted together, a decision of whether to transmit the whole observation vector or not has to be made, for instance due the limited power or wireless channel occupancy constraints.

3.4 Reward Shaping

Reward shaping is a popular approach to direct RL agents towards a desired goal. Here, we want the agent not only move towards to the original goal (which is encouraged by the original reward r), we also want it to learn to control β_t^i so that not all samples are taken with the same accuracy. Hence, we propose reward shaping in the following form:

$$\tilde{r}_t = f(r_t, \beta_t) \tag{7}$$

where r_t is the original reward, $\tilde{r}_t$ is the new modified reward and $f(r_t, \beta_t)$ is a monotonically non-decreasing function of r_t and β_t^i, $\forall i$. Hence, the agent not only tries to maximize average of the original reward but it also tries to maximize the "inaccuracy" of the measurements. This can be

equivalently interpreted as minimizing the cost due to accurate measurements. In the case where there is a direct cost function $c^i(.)$ that increases with the accuracy of the observation o^i (see, for instance, the example in Section A.1 where transmission power can be interpreted as the direct cost), the following additive form can be used

$$\tilde{r}_t = r_t - \lambda \sum_{i=1}^{n} c^i(\beta_t^i), \tag{8}$$

where $c^i(\beta_t^i)$ is a non-increasing function of β_t^i and $\lambda \geq 0$ is a weighting parameter. Hence, the agent's aim is to maximize the original reward as well as minimize the cost of the observations.

4 EXPERIMENTS

4.1 SETTING

Observation Models: We consider the following environments: MountainCarContinuous-v0, Pendulum-v0, CartPole-v1 from the OpenAI Gym (Brockman et al., 2016). We now illustrate how the modified environment with noisy observations is obtained using the mountain car environment. The details and the parameter values for all environments can be found in the Appendix A.2.

We first illustrate Scenario A and then Scenario B. The original observations of MountainCarContinuous-v0 are the position x_t and the velocity $\dot{x}_t$. In our framework, the agent has access to noisy versions of these original observations

$$\tilde{x}_t = x_t + Q_x \times \Delta x_t(\beta_t^1), \tag{9a}$$

$$\tilde{\dot{x}}_t = \dot{x}_t + Q_{\dot{x}} \times \Delta \dot{x}_t(\beta_t^2), \tag{9b}$$

where $\Delta x_t(\beta_t^1) \sim \mathcal{U}(-\beta_t^1, \beta_t^1)$ and $\Delta \dot{x}_t(\beta_t^2) \sim \mathcal{U}(-\beta_t^2, \beta_t^2)$ with $\mathcal{U}(-\beta, \beta)$ denoting the uniform distribution over $[-\beta, \beta]$. The noise variables are stat. ind., in particular $\Delta x_t(\beta_t^1)$ and $\Delta \dot{x}_t(\beta_t^2)$ are stat. ind. from each other and also stat. ind. over time. Here, Q_x and $Q_{\dot{x}}$ determine the ranges of the noise level and they are set as the 0.1 times of the full range of the corresponding observation, i.e., $Q_x = 0.18$ and $Q_{\dot{x}} = 0.014$.

Our agent chooses $\beta_t^i \in [0, 1]$ in addition to the original action of the environment, i.e. the force a_t that would be exerted on the car. The original reward of the environment per step is given by $r_t = -0.1 \times a_t^2$. The reward is shaped using an additive model

$$\tilde{r}_t = r_t + \kappa_A \times \left(\frac{1}{n} \sum_{i=1}^{n} \beta_t^i \right), \tag{10}$$

where $n = 2$ and $\kappa_A > 0$ is chosen as 5×10^{-6}. The original environment has also a termination reward which the agent gets when the car passes the target position at 0.45, which is also provided to our agent upon successful termination.

In Scenario B, at each time instant we either have no observations or we obtain the original observation vector, i.e. $\tilde{x}_t = x_t$ and $\tilde{\dot{x}}_t = \dot{x}_t$. These cases correspond to $\bar{\beta}_t = \infty$ and $\bar{\beta}_t = 0$, respectively. The reward function is given as $\tilde{r}_t = r_t + \kappa_B \times g(\bar{\beta}_t)$ where $\kappa_B = -0.5$ and $g(\bar{\beta}_t) = -1$ for $\bar{\beta}_t = 0$, and 0 otherwise. In the implementation, we have mapped ∞ to 1, i.e. the decision variable is $\bar{\beta}_t \in \{0, 1\}$, hence $\bar{\beta}_t = 1$ corresponds to not obtaining a sample in Scenario B.

RL algorithm: For the RL algorithm, we adopt a deep RL setting, combining reinforcement learning with deep learning using the policy-based approach Trust Region Policy Optimization (TRPO) (Schulman et al., 2015; Hill et al., 2018). The parameters are kept constant for all experiments and are provided in Appendix A.3. For Scenario A, the noisy samples are fed to the algorithm. For Scenario B, the last acquired sample is used.

Plots: Unless otherwise stated, all results are reported are averages (such as average cumulative rewards and average β_t^i) using 1000 episodes. For the plots, observation space is mapped to a grid with uniform intervals. Averages are taken with respect to the number of visits to each given observation state range. For example, for Scenario A the average of β_t^i when $\tilde{x}_t \in [-0.1, +0.1]$ is shown as one average value at the center 0. For Scenario B, we report the sample skip frequency,

Table 1: Comparison of the average returns

ENVIRONMENT	ORIGINAL	A	B
MOUNTAINCARCONTINUOUS-V0	94	94	94
PENDULUM-V0	-152	-158	-170
CARTPOLE-V1	494	482	472

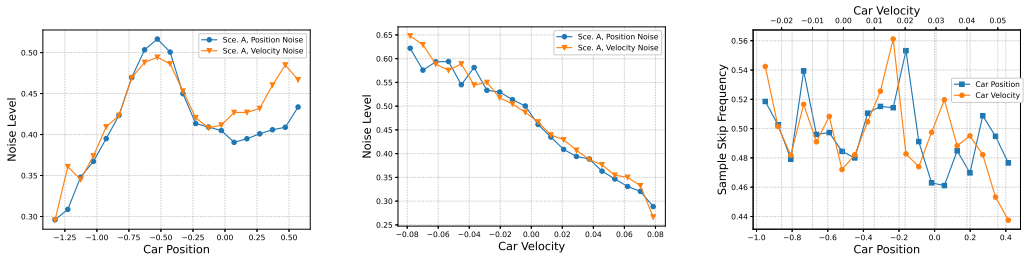

(a) Scenario A, noise levels vs $\tilde{x}_t$ (b) Scenario A, noise levels vs $\tilde{\dot{x}}_t$ (c) Scenario B

Figure 1: Mountain car, noise levels or sample skip frequency versus one observation type

i.e. the number of times the agent decided not to acquire a new observation when the last observed state of the agent falls into a given interval, such as for $\tilde{x} \in [-0.1, +0.1]$ as one value at 0. In all 2-D plots, the pink color indicates there was no visit to that observation state.

4.2 OVERVIEW

We benchmark our results against the performance of the agent that use the original observations, and trained using the same RL algorithm. The resulting average cumulative rewards in terms of r_t are presented in Table 1. We present the reward corresponding only to the original task so that we can evaluate the success of the agent in this task. These results illustrate that the agent can learn to adjust the accuracy level and still obtain successful performance. For Mountain car environment all agents have the same average return and for the others, the agents working with the noisy or skipped observations have a slightly weaker performance but still achieve the task of bringing/keeping the pendulum/pole in a vertical position in a reasonable number of time steps.

We now focus on the data collection strategies chosen by the agent for the mountain car and pendulum environments. The results for the other environments are provided in Appendix A.4 due to page limitations.

4.3 MOUNTAIN CAR

The chosen noise levels and the sample skip frequencies for Mountain Car are presented in Figure 1-2 and Figure 2c. In the mountain car environment, the car starts randomly around position -0.5 and it has to first go in the reverse direction (corresponding to a negative velocity) to climb the hill located around position -1.25 in order to gain momentum and climb to hill at the right (corresponding to a positive velocity) and reach the target location 0.45 which is at the top of this hill. The results reflect the possible observation trade-offs in this strategy:

Figure 1a, shows that most noisy observations in position and velocity (Scenario A) are preferred around -0.5 (where the car position is initialized), and the most accurate samples are taken when the car is around position -1.2. This is the position where the car has to make sure that it has reached to the top of the left hill so that it has enough momentum to climb the right hill. In the case of the dependence of the noise level on the velocity, Figure 1b shows that accurate samples are preferred when the velocity has high positive values.

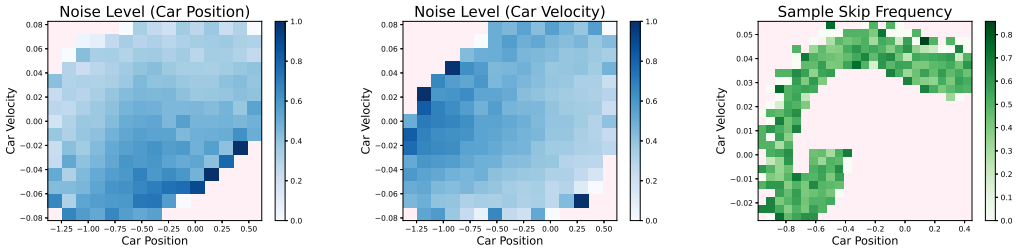

(a) Scenario A, position noise (b) Scenario A, velocity noise (c) Scenario B

Figure 2: Mountain car, noise levels or skip frequencies over the whole observation space

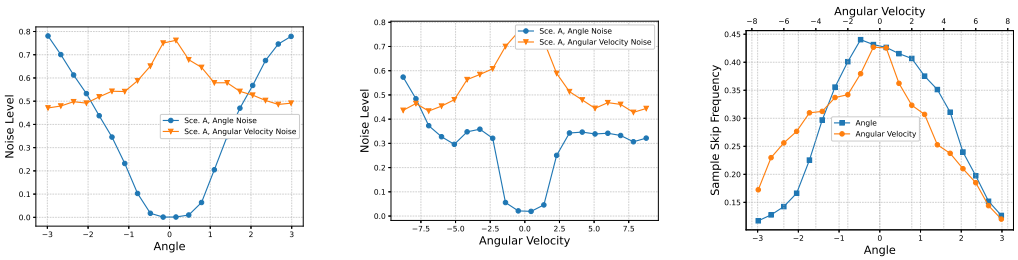

(a) Scenario A, noise levels vs $\tilde{\theta}$ (b) Scenario A, noise levels vs $\tilde{\dot{\theta}}$ (c) Scenario B

Figure 3: Pendulum, noise levels or sample skip frequency versus one observation type

Figure 1c shows that approximately half of the samples are dropped in Scenario B regardless of the observation state, suggesting a high inherent sampling rate in the environment. This difference in the behaviour with the noisy and skipped observations illustrates the fundamental difference in these frameworks. In the case of noisy observations, the agent has to discover that the observations are uncertain and counteract this uncertainty. On the other hand, when taking perfect observations are possible, as in the case of Scenario B, the agent can internalize the exact environment dynamics (since mountain car environment has no inherent noise in its observations) and determine its exact state using the previous observed state and its action.

Comparing Figure 2 and Figure 2c, we observe that in the case of noisy observations a larger part of observation space is visited, which is partly due the fact that the plots are drawn according to the observations acquired by the agent and not the true states. Note that this does not affect the performance in the original task, as illustrated in Table 1.

4.4 PENDULUM

The results for the pendulum are presented in Figure 3-4 and Figure 4c. Here, the task is to keep the pendulum at a vertical position, corresponding to an angle of 0. Figure 3a and Figure 4a show that observations with low position (i.e. angle) noise (Scenario A) is preferred when the pendulum is close to the vertical position and has relatively small angular velocity. On the other hand, when the samples can be completely skipped (Scenario B), the agent skips a large ratio of the samples in this region, as shown in Figure 3a and Figure 4a. Note that the agent spends most of the episode in this target region in the vertical position. Here, the agent prefers noiseless samples since a noisy sample may cause the control policy to choose a wild movement which might destabilize the pendulum. On the other hand, the agent may safely skip some samples at the upright position as the last sample is very close to current one because the angular velocity is too low.

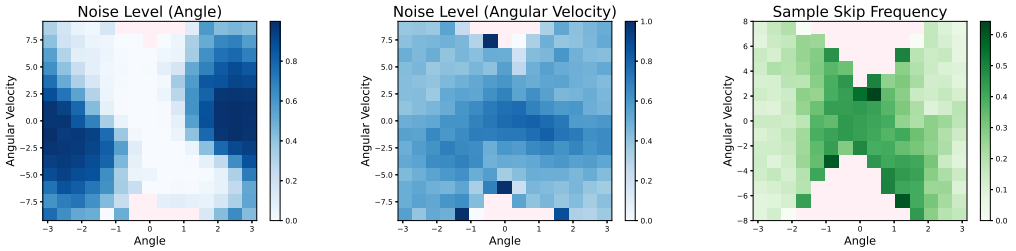

(a) Scenario A, position noise (b) Scenario A, velocity noise (c) Scenario B

Figure 4: Pendulum, noise levels or skip frequencies over the whole observation space

5 Discussion and Conclusions

We have proposed a framework for revealing the information structure of the observation space in a systematic manner. We have adopted a reinforcement learning approach which utilizes a cost function which increases with the accuracy of the observations. Our results uncover the relative usefulness of different types of observations and trade-offs within; and provide insights for further design of active data acquisition schemes for autonomous decision making. Further discussion of our results and some research directions are as follows:

- Our results illustrate that settings with the inaccurate observations and skipped observations should be treated differently since the type of uncertainty that the agent has to counteract in these settings are inherently different.
- Strategies for processing of the noisy/skipped observations should be investigated. Questions such as the following rise: " Should all the processing be off-loaded to the RL agent or should pre-processing of observations be performed, similiar to Kalman filtering in the case of linear control under linear state space models Ljung (1999)?", "How does the answer to the former question depend on the RL approach, the environment and observation models?"
- Our results suggest that inherent sampling rate of some of the standard RL environments may be higher than needed (for instance, see the Mountain Car example), indicating yet-another reason why some of these environments are seen as unchallenging for most-of-the state-of-art RL algorithms.
- We have provided a quantification of the sensitivity of the agents performance to noisy/skipped observations at different observation regions illustrating that this sensitivity can be quite different based on the observation region. Utilizing this information for supporting robust designs as well as preparing adversarial examples is an interesting line of future research.

REFERENCES

Ershad Banijamali, Rui Shu, Mohammad Ghavamzadeh, Hung Hai Bui, and Ali Ghodsi. Robust locally-linear controllable embedding. *Inter. Conf. on Artificial Intelligence and Statistics, AISTATS*, 84:1751–1759, 2018.

Marc Bellemare, Sriram Srinivasan, Georg Ostrovski, Tom Schaul, David Saxton, and Remi Munos. Unifying count-based exploration and intrinsic motivation. *Advances in Neural Information Processing Systems*, pp. 1471–1479, 2016.

J. Boedecker, J. T. Springenberg, J. Wülfing, and M. Riedmiller. Approximate real-time optimal control based on sparse gaussian process models. In *2014 IEEE Symp. on Adaptive Dynamic Program. and Reinforcement Learning (ADPRL)*, 2014.

Greg Brockman, Vicki Cheung, Ludwig Pettersson, Jonas Schneider, John Schulman, Jie Tang, and Wojciech Zaremba. Openai gym, 2016.

Kurtland Chua, Roberto Calandra, Rowan McAllister, and Sergey Levine. Deep reinforcement learning in a handful of trials using probabilistic dynamics models. In *Adv. in Neural Information Processing Systems 31*, pp. 4754–4765. 2018.

Thomas M. Cover and Joy A. Thomas. *Elements of Information Theory*. Wiley, 1991.

Marc Peter Deisenroth and Carl Edward Rasmussen. PILCO: A Model-Based and Data-Efficient Approach to Policy Search. *Proc. of the International Conference on Machine Learning*, 2011.

Pinar Donmez, Jaime G. Carbonell, and Jeff G. Schneider. A probabilistic framework to learn from multiple annotators with time-varying accuracy. In *Proc. of the SIAM International Conference on Data Mining*, pp. 826–837, 2010.

Yarin Gal, Rowan McAllister, and Carl Edward Rasmussen. Improving PILCO with Bayesian neural network dynamics models. In *Data-Efficient Machine Learning workshop, ICML*, 2016.

Andrea Goldsmith. *Wireless Communications*. Cambridge University Press, 2005.

Danijar Hafner, Timothy Lillicrap, Ian Fischer, Ruben Villegas, David Ha, Honglak Lee, and James Davidson. Learning latent dynamics for planning from pixels. *Proceedings of Machine Learning Research*, 97:2555–2565, 2019.

Mikael Henaff, William F. Whitney, and Yann LeCun. Model-based planning with discrete and continuous actions, 2018.

Ashley Hill, Antonin Raffin, Maximilian Ernestus, Adam Gleave, Anssi Kanervisto, Rene Traore, Prafulla Dhariwal, Christopher Hesse, Oleg Klimov, Alex Nichol, Matthias Plappert, Alec Radford, John Schulman, Szymon Sidor, and Yuhuai Wu. Stable baselines. `https://github.com/hill-a/stable-baselines`, 2018.

Lennart Ljung. *System Identification*. Prentice-Hall, 1999.

Manuel Lopes, Francisco S. Melo, and Luis Montesano. Active learning for reward estimation in inverse reinforcement learning. In *European Conference on Machine Learning and Knowledge Discovery in Databases, ECML*, pp. 31–46, 2009.

Shakir Mohamed and Danilo J. Rezende. Variational information maximisation for intrinsically motivated reinforcement learning. pp. 2125–2133, 2015.

Deepak Pathak, Pulkit Agrawal, Alexei A. Efros, and Trevor Darrell. Curiosity-driven exploration by self-supervised prediction. In *Proc. of the International Conference on Machine Learning*, pp. 2778–2787, 2017.

John Schulman, Sergey Levine, Pieter Abbeel, Michael I. Jordan, and Philipp Moritz. Trust region policy optimization. In *Proc. of the 32nd International Conference on Machine Learning*, pp. 1889–1897, 2015.

Sarah Schwöbel, Stefan Kiebel, and Dimitrije Markovic. Active Inference, Belief Propagation, and the Bethe Approximation. *Neural Computation*, 30(9):2530–2567, September 2018.

Burr Settles. From theories to queries: Active learning in practice. In *Active Learning and Experimental Design workshop - AISTATS*, 2010.

Susanne Still and Doina Precup. An information-theoretic approach to curiosity-driven reinforcement learning. *Theory of Bioscience*, 131(3):139–148, 2012.

Kai Ueltzhöffer. Deep Active Inference. *Biological Cybernetics*, 112(6):547–573, December 2018.

Manuel Watter, Jost Tobias Springenberg, Joschka Boedecker, and Martin A. Riedmiller. Embed to control: A locally linear latent dynamics model for control from raw images. In *Advances in Neural Information Processing Systems*, pp. 2746–2754, 2015.

A APPENDIX

A.1 EXAMPLE: WIRELESS COMMUNICATIONS

We now provide a motivating example to illustrate how observations can have a cost that is increasing with the accuracy and the decision maker can choose this accuracy level.

A standard model for single terminal wireless communications is the additive white Gaussian noise (AWGN) channel (Goldsmith, 2005; Cover & Thomas, 1991)

$$y_t = x_t + v_t \tag{11}$$

where x_t represents the channel input (i.e. message at the transmitter) at time t, y_t represents the corresponding channel output (i.e. the observation at the receiver) and the white Gaussian random process v_t represents the channel noise. The capacity of this channel, i.e. the maximum number of information bits that can be sent, is determined by the signal-to-noise ratio (SNR), i.e. the average power in x_t divided by the average power in v_t. In particular, the capacity is given by (Goldsmith, 2005; Cover & Thomas, 1991)

$$C = \log_2(1 + \frac{P_x}{P_v}) \tag{12}$$

where P_x and P_v are the average power levels of x_t and v_t, respectively. Hence, the capacity increases with P_x. On the other hand, one cannot use a very high value of P_x since broadcasting at high power levels is costly. In particular, P_x directly contributes to the actual power required by the transmitter. Note that P_x controls the accuracy of the observations. In particular, by dividing both sides by $\sqrt{P_x}$, (11) can be equivalently represented as

$$\bar{y}_t = \bar{x}_t + \bar{v}_t \tag{13}$$

where $\bar{y}_t \triangleq \frac{1}{\sqrt{P_x}} y_t$, $\bar{x}_t \triangleq \frac{1}{\sqrt{P_x}} x_t$ and $\bar{v}_t \triangleq \frac{1}{\sqrt{P_x}} v_t$. The average power of $\bar{x}_t$ is 1 and average power of $\bar{v}_t$ is P_v/P_x. The SNR, and hence, the channel capacity are the same in (11) and (13) and hence these representations are equivalent for all relevant purposes. In particular, determining P_x directly determines the effective noise level. With v_t Gaussian, we have $v_t \sim \mathcal{N}(0, P_v)$. Hence, the conditional distribution of the observations $\bar{y}_t$ is given by $p(\bar{y}_t|\bar{x}_t) = \mathcal{N}(\bar{x}_t, P_v/P_x)$ where P_v/P_x can be chosen as β_t. Hence, as the accuracy of the observations increases (P_v/P_x decreases), the cost of the observations (P_x) increases. In this context, several interesting questions that relates to the accuracy of the observations and the power cost can be posed, for instance how to distribute a certain total power budget P_{total} over channels $y_t^i = x_t^i + v_t^i$ with different intrinsic power levels P_{v_i} ().

This example illustrates the basic premise of our problem setting in a practical scenario; a decision maker who can adjust the noise levels of the observations which has a cost associated with them. It also suggests that the constraints on the wireless communications constitute a general and potential hindrance in remote control applications. Consider a device that makes the observations and takes actions but gets its commands (i.e. decisions about which actions to take) from another decision unit, such as the control of a robot or a drone by a remotely run RL algorithm which is controlling a large number of such units. Here, it is beneficial to consider policies that can work with inaccurate observations since sending accurate measurements are costly from a power perspective, which will be particularly important for a device with a limited battery, such as a drone flying at a remote location. Similarly, if the wireless communication channel cannot be used at all times, for instance, due to the limited bandwidth available, RL methods that can utilize the limited communication resources efficiently and optimize performance under such conditions are needed.

A.2 ENVIRONMENT PARAMETERS

In this section, we provide the modified parameters for all the environments in the experiments. Consider a generic environment with the observation variables o_t^i, where o_t^i denotes the ith observation variable at time t. The limited-accuracy observations $\tilde{o}_t^t$ are obtained using

$$\tilde{o}_t^i = o_t^i + Q^i \times \Delta o_t^i(\beta_t^i) \tag{14}$$

where $\Delta o_t^i \sim \mathcal{U}(-\beta_t, \beta_t)$. We choose $Q^1 = 0.1$ and $Q^2 = 0.2$ for the Pendulum-v0, $Q^i = 0.2$ for the CartPole-v1, and $Q^i = 0.1$ for the MountainCarContinuous-v0. The ordering of the observations

Table 2: Environment parameters, reward weighting for different scenarios

ENVIRONMENT	κ_A, κ_B
MOUNTAINCARCONTINUOUS-V0	$5 \times 10^{-6}, 0.5$
PENDULUM-V0	$1, 0.2$
CARTPOLE-V1	$0.2, 0.04$

Table 3: Hyperparameters of the TRPO algorithm

PARAMETER	VALUE
GRADIENT DAMPENING FACTOR	2.35E-05
WEIGHT FOR THE ENTROPY LOSS	0.01118
GAMMA	0.98
GAE FACTOR	0.9
KULLBACK-LEIBLER LOSS THRESHOLD	0.000193
NO. OF TIMESTEPS TO RUN PER BATCH	1024
NO. ITERS. FOR LEARNING FOR VALUE FUNC	10
STEPSIZE OF VALUE FUNC.	0.00428

is the same with the ones provided in OpenAI Gym (Brockman et al., 2016). For instance, for MountainCarContinuous-v0 car position and car velocity correspond to o^1 and o^2, respectively. Note that indices start with $i = 0$ in OpenAI Gym whereas here we start with $i = 1$. For Scenario A-II and Scenario B, observation parameters and reward definitions are handled in the same manner with the MountainCarContinousV0 presented in Section 4.1.

The reward function under Scenario A is given by

$$\tilde{r}_t = r_t + \kappa_A \times \left(\frac{1}{n} \sum_{i=1}^{n} \beta_t^i \right), \tag{15}$$

where r_t is the original reward and $\kappa_A > 0$. For Scenario B is given by $\tilde{r}_t = r_t + \kappa_B \times g(\bar{\beta}_t)$ where $g(\bar{\beta}_t) = -1$ for $\bar{\beta}_t = 0$, and 0 otherwise. The associated κ values for different environments are presented in Table 2.

A.3 TRPO PARAMETERS

The same TRPO parameters are used in all experiments. These are provided in Table 3.

A.4 ADDITIONAL RESULTS

We now provide the results for the cart pole environment in Figure 5-8, which were not included in the main text due to page limitations. For the sake of brevity, the noise levels over observations pairs is only provided for the position noise levels whereas averages are provided for all observation types.

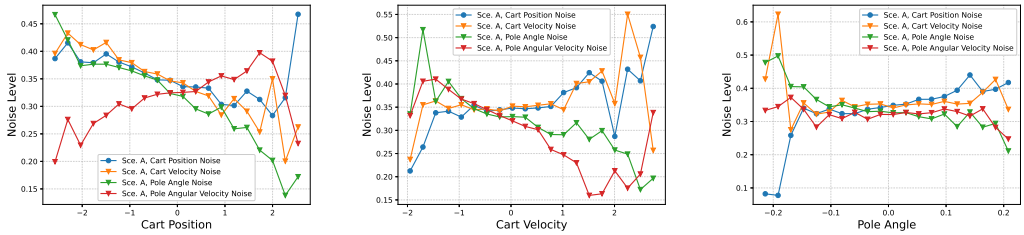

(a) Scenario A, noise vs position (b) Scenario A, noise vs velocity (c) Scenario A, noise vs angle

Figure 5: Cart pole, noise levels versus one observation type

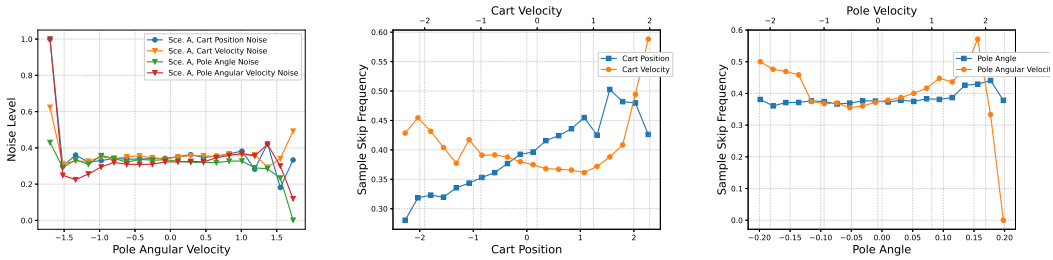

(a) Scenario A, noise vs angular velocity (b) Scenario B, sampling frequency vs position and velocity (c) Scenario B, sampling frequency vs angle and angular frequency

Figure 6: Cart pole, noise levels or sample skip frequency versus one observation type

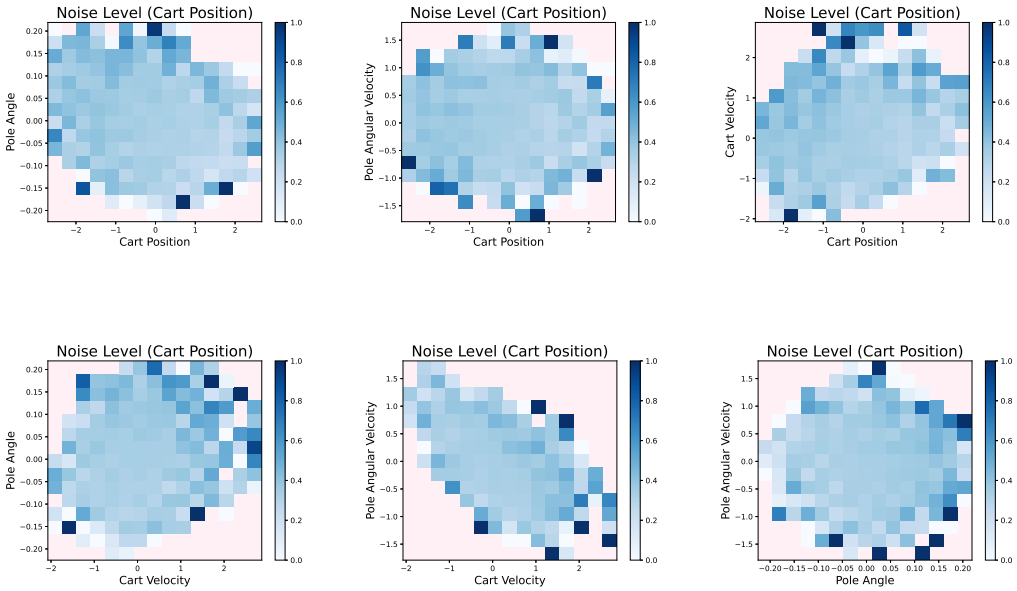

Figure 7: Cart Pole, Scenario A, noise levels for the position over the pairs of the observation variables

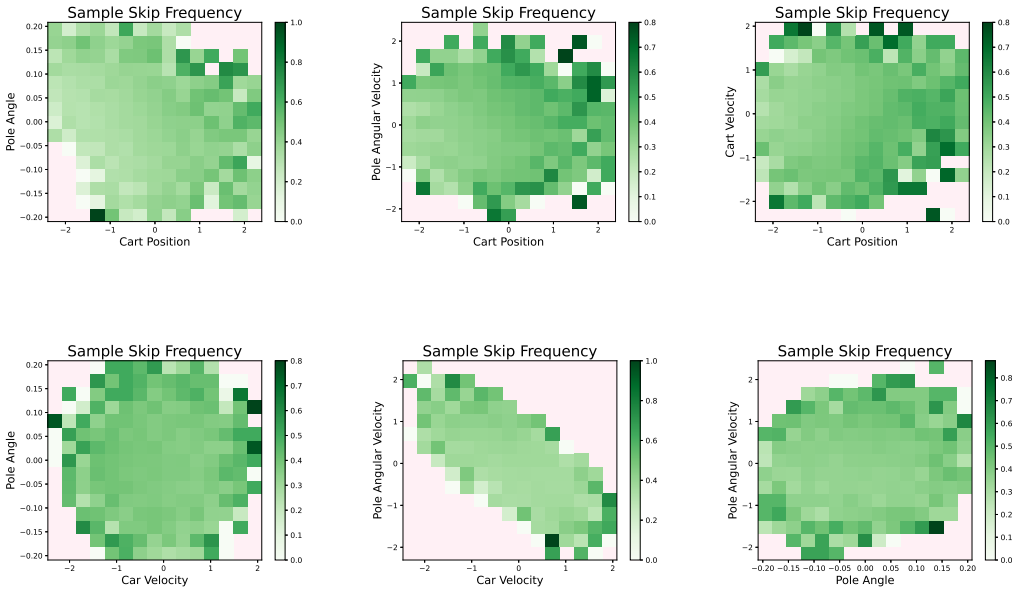

Figure 8: Cart Pole, Scenario B, sample skip frequencies over the pairs of the observation variables